Minireview

Predicted structure and possible ionmotive mechanism of the sodium-linked NADH-ubiquinone oxidoreductase of *Vibrio alginolyticus*

Peter R. Rich[a,*], Brigitte Meunier[a], F. Bruce Ward[b]

[a]*Glynn Research Foundation, Bodmin, Cornwall PL30 4AU, UK*
[b]*Institute for Cell and Molecular Biology, Edinburgh University, Edinburgh, UK*

Received 2 October 1995

Abstract Two groups have now published sequences of the six genes contained in the operon coding for the sodium-linked NADH-ubiquinone oxidoreductase of *Vibrio alginolyticus*. Sequence analyses indicate that this enzyme is unrelated to other known respiratory NADH dehydrogenases. A search for cofactor motifs suggests that the enzyme contains only one FAD, a ferredoxin-type iron sulphur centre, and the NADH-binding site. These are all located on NqrF, a subunit that can be recognized as a new member of a large diverse family of NAD(P)H-oxidizing flavoenzymes. A possible model of ion-coupling is presented, based upon this new information.

Key words: NADH-ubiquinone oxidoreductase; NADH dehydrogenase; Sodium ion translocation

1. Background

Several types of enzyme (NQR) are known to catalyse the respiratory reaction of oxidation of NADH by membrane-bound ubiquinone. Only one, termed complex I, is found in mammalian mitochondria, where it oxidizes internally generated NADH. Bovine complex I is remarkably complicated, with seven mitochondrially encoded and at least 34 further nuclear encoded subunits [1]. Gene clusters coding for proton translocating NADH-ubiquinone oxidoreductases have also been identified in the prokaryotes *Paracoccus denitrificans*, *Rhodobacter capsulatus* and *Escherichia coli* [2–4]. These comprise homologues of only 14 of the mammalian subunits [5] and, presumably, represent a more minimal core catalytic structure. The purified enzyme from *E. coli* can be subfractionated into three domains, viz. a fragment (FP) of three subunits which contains the NADH site, FMN and iron sulphur centres; a more amphipathic fragment (IP) of four subunits also containing iron sulphur centres; and a very hydrophobic fragment (HP) of seven proteins which are homologues of the mitochondrially encoded subunits of eukaryotes. In the mitochondrial enzyme, one HP subunit (ND1) contains a ubiquinone-binding site while another (ND2) is reactive with rotenone and DCCD [1]. All homologues of complex I are presumed to be coupled to proton translocation and have been generically termed NDH-1 types [5,6].

*Corresponding author. Fax: (44) (1208) 821 575.
E-mail: mbprr@seqnet.dl.ac.uk

Two other types of NADH dehydrogenase can be found in mitochondria from fungal and plant sources [7]. One of these oxidizes internally generated NADH but, in contrast to complex I, it is not coupled to proton translocation. It is likely to be homologous to a non-protonmotive NQR in bacteria, termed NDH-2 [6]. The enzyme may be a single polypeptide, whose sequence has been established [8–10], and with FAD as the only redox cofactor [6]. A third NADH dehydrogenase in the inner membrane of plant and fungal mitochondria, which we propose might be termed NDH-3, has an externally facing NADH site and can directly oxidize cytosolic NADH [11]. This enzyme is also not coupled to proton translocation [12]. A bacterial homologue has not been identified and its detailed structure and composition remain unknown.

A further type of NQR was first found in the marine bacterium *Vibrio alginolyticus*, an organism which produces an electrochemical gradient of sodium ions in aerobic respiration. The enzyme is induced at alkaline pH and is coupled to sodium ion translocation [13–15]. Substantial evidence has been accumulated that this is the result of a primary coupling of electron transfer and sodium ion translocation, rather than to a secondary sodium/proton antiport system [16,17]. This Na^+–NQR appeared to be distinct from NDH-1, NDH-2 and NDH-3 on the basis of its sodium ion dependency, inhibitor (especially silver ion) sensitivity, NADH analogue specificity, and polypeptide and cofactor composition [18–20]. Early biochemical studies had indicated that the purified Na^+–NQR complex was composed of only three subunits, α, β and γ, with apparent molecular masses of 52, 46 and 32 kDa, respectively, and containing only FAD and FMN as redox cofactors. A possible mechanism of ion-coupling was proposed on this basis [18]. However, the operon encoding these subunits has now been sequenced by two groups and six open reading frames (ORFs) have been identified [21–23]. It is, therefore, timely to reassess the possible structure and mechanism of this unusual member of the NQR family of enzymes.

2. Analyses of amino acid sequences

2.1. Assignment of ORFs

The general features of the polypeptides encoded by the six ORFs are summarized in Table 1. These genes have been termed *nqra–nqrf*, based upon their arrangement in the operon. By comparison with N-terminal sequence data and M_r values obtained from subunits separated by SDS-PAGE, we can as-

SSDI 0014-5793(95)01164-1

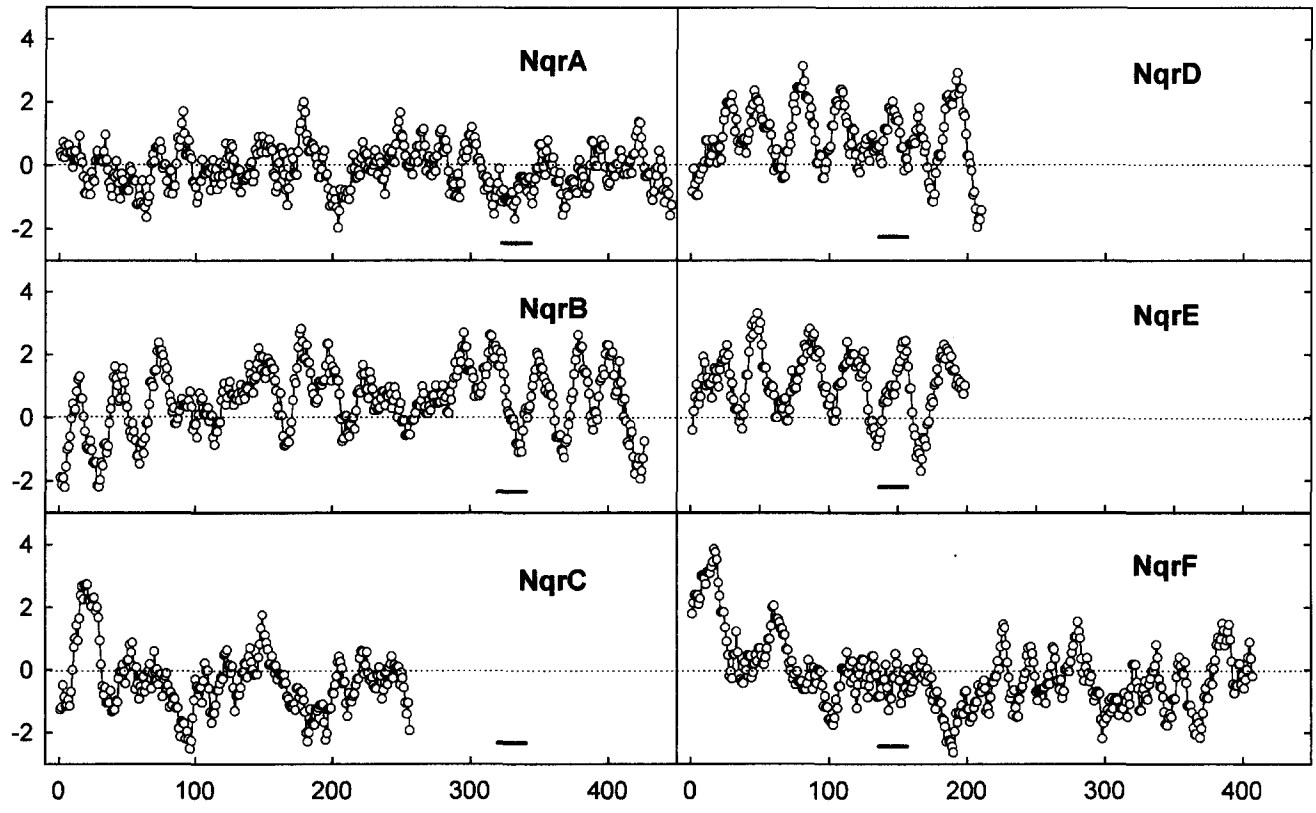

Fig. 1. Hydropathy plots of deduced amino acid sequences. Plots were generated with a Modified Chou-Fasman Secondary Structure Predictor program (version 1.00) supplied by A.R. Crofts (University of Illinois), using a modified Rao-Argos index with a span of 11 amino acids.

cribe the NqrA and NqrC to the α and γ subunits, respectively (in our enzyme preparations, the band attributed to the γ subunit might have been a pair of bands and so we have labelled it as $\gamma 2$). From further sequence analyses (below), it is apparent that NqrF is equivalent to the NADH-oxidizing β subunit of the original enzyme preparations [18].

nqrf is followed by a transcription stop signal, a polydT tail and a further 293 bp of non-coding DNA [23]. The identities of ORFs downstream of this region have yet to be established. It has recently been reported that the second of these shows homology with sodium/proton antiporters but is distinct from the one which has been sequenced in *V. alginolyticus* [24]. Whether the gene products of these additional ORFs are relevant to the structure/mechanism of the Na^+–NQR remains unknown.

2.2. Hydropathy plots

Hydropathy plots (Fig. 1) indicate that NqrA, NqrC and NqrF are the least hydrophobic of the six subunits with 0, 1 and 2 predicted membrane-spanning α-helices, respectively. The other three subunits (NqrB, NqrD and NqrE) are substantially more hydrophobic, with 6–12, 4–7 and 6 predicted membrane-

Table 1
Summary of the predicted properties of proteins encoded by the operon of the sodiummotive NADH-ubiquinone oxidoreductase of *V. alginolyticus*

	M_r	No. residues	*pI*	N-terminus	Probable no. of membrane-spanning helices	Comments
NqrA	48 622	446	5.58	MITIKKGLDL-	0	Equivalent to α subunit
NqrB	48 809	426	9.12	MPRYYREGRV-	6–12	Very hydrophobic
NqrC	27 703	256	4.82	MASNNDSIKK-	1 (N-terminal)	Equivalent to $\gamma 2$ subunit; hyrophobic N-terminal region
NqrD	22 602	210	9.28	MSSAQNVKKS-	4–7	Very hydrophobic
NqrE	21 540	198	7.18	MEHYISLLVK-	6	Very hydrophobic
NqrF	45 274	407	4.54	MDIILGVVMF-	2 (N-terminal)	Equivalent to β subunit; hydrophobic N-terminal region; binding motifs for [4Fe-4S], FAD and NADH

Sequences of subunits were derived from the following sources: NqrA–NqrD, Beattie et al. [21] and with the change of a single residue R to W in NqrC as suggested in [22], NqrE, Hayashi et al. [22], NqrF, Tan et al. [23]. Arrangement of genes on DNA: ...bol A...*nqra...nqrb...nqrc...nqrd...nqre...nqrf*...stop signal...polydT...

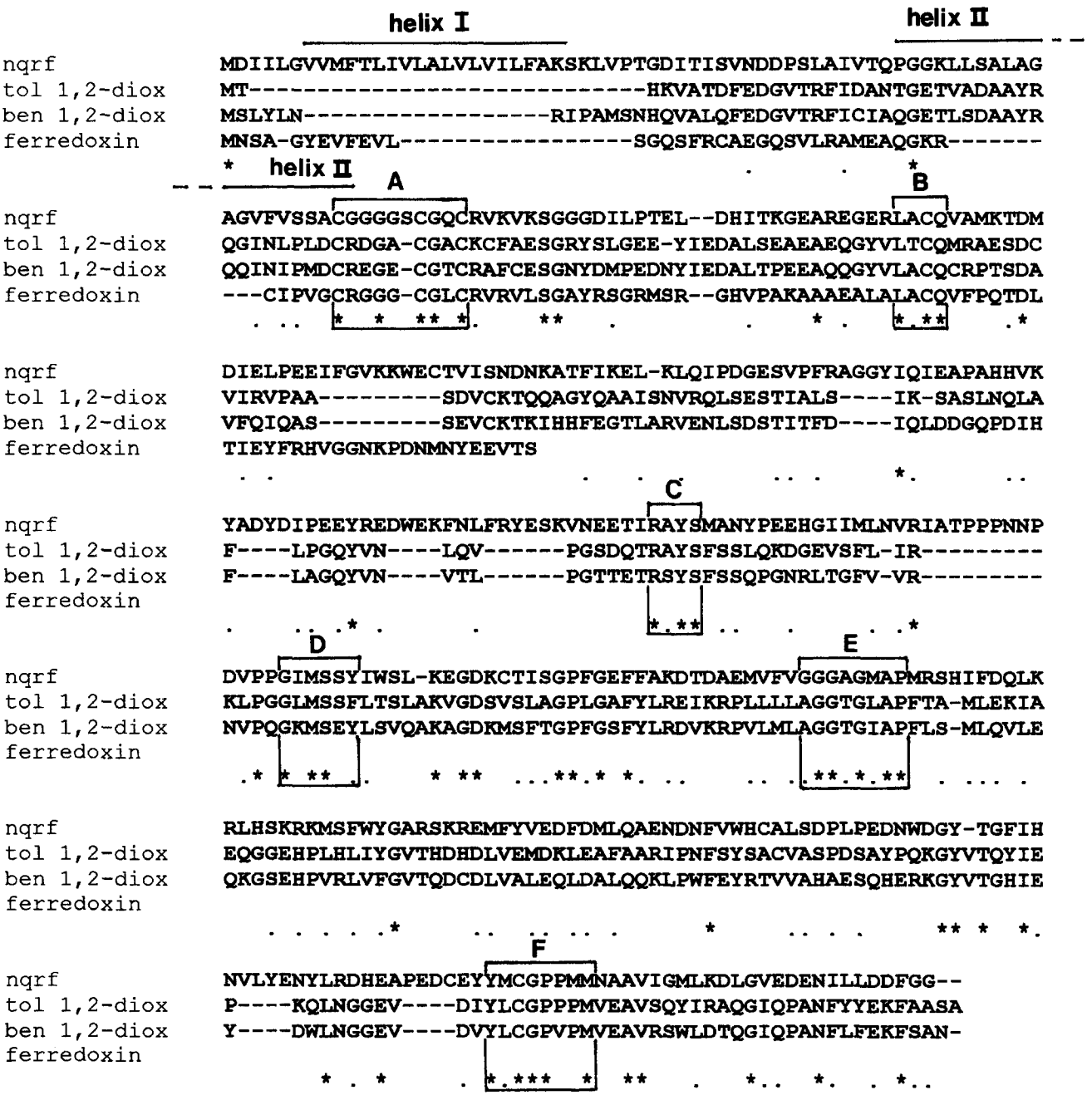

Fig. 2. Sequence alignments of NqrF, toluate 1,2-dioxygenase, benzoate 1,2-dioxygenase and ferredoxin. Sequences of toluate 1,2-dioxygenase from *P. putida* [39], benzoate 1,2-dioxygenase from *Acinebacter calcoaceticus* [40] and ferredoxin from *P. putida* [41] were aligned against the sequence of NqrF [23] using the program CLUSTALV [42] (protein weight matrix PAM 250; fixed and floating gap penalty 10). The predicted positions of two membrane-spanning α-helices of NqrF are shown as bars labelled helices I and II. Boxed regions contain possible residues involved in the binding of a ferredoxin-like [4Fe-4S] iron sulphur centre (boxes A and B), FAD (boxes C and D) and NADH (boxes E and F).

spanning helices, respectively. Since hydrophobic proteins are known to run poorly on SDS-PAGE gels, it seems possible that these subunits were present but undetected in purified enzyme preparations. Alternatively, it may be that the enzyme, like complex I, easily fragments into the equivalent of a relatively hydrophilic FP portion with NADH dehydrogenase activity and a more hydrophobic HP portion which is lost on purification.

2.3. *Sequence homologies with other proteins and cofactor-binding motifs*

Sequence comparisons were performed between the deduced sequences of the proteins encoded by the genes *nqra–nqrf* and proteins in the SWISSPROT database, using the program FASTA to determine homology. Comparisons were also made with the subunits of a bacterial NDH-1 [25–29] and the bacterial form of NDH-2 from *E. coli* [8] using the program

BESTFIT. In addition, the three hydrophobic proteins encoded by *nqrb*, *nqrd* and *nqre* were compared with bacterial Na^+/H^+ antiporters [24,30–32]. Significant homologies with proteins in the SWISSPROT database were found only in the case of the NqrF subunit and this arose primarily from the presence of common binding motifs for NADH, FAD and the iron sulphur centre (see below). Our initial comparisons suggested possible weak homologies of two of the hydrophobic subunits with hydrophobic subunits of complex I and with sodium/proton antiporters. However, further tests of signficance by comparison of randomized sequences showed that the matching was little better than chance and was likely to have arisen solely because of the hydrophobic characters of the proteins.

We further searched the deduced amino acid sequences of NqrA-NqrF for possible cofactor-binding motifs and have found compelling evidence for such motifs only in NqrF, and it is the regions around these motifs which accounts for the homologies identified in the overall sequence comparisons above. The N-terminal region of NqrF shows strong homology with ferredoxin and with a variety of NAD(P)H-oxidizing enzymes which also contain a [4Fe-4S] iron sulphur centre. The C-terminal part of NqrF also shows clear local regions of homology that may be identified with sites for binding FAD and NAD(P)H in these same NAD(P)H-oxidizing enzymes. These enzymes are all members of a large family of flavoenzymes related to ferredoxin reductase (FNR) [33] which includes, e.g. phenol hydroxylase P5 protein, xylene monooxygenase, toluate 1,2-dioxygenase, benzoate 1,2-dioxygenase, CDP-6-deoxy-3,4-glucoseen reductase and methane monooxygenase component C. Most importantly, a number of crystal structures are available for interpretation of conserved regions [34,35].

The important points concerning NqrF are illustrated in Fig. 2, where its deduced amino acid sequence has been aligned with those of ferredoxin and toluate and benzoate 1,2-dioxygenase. Immediately following the two predicted membrane-spanning α-helices in the N-terminal region of NqrF (labelled helices I and II in Fig. 2) is the motif C_{69}-(x_5)-C_{75}-(x_2)-C_{78} (box A in Fig. 2) and, after a spacing of 30 amino acid residues, a further sequence of L_{108}ACQ (box B), indicating the presence of a [4Fe-4S] iron sulphur centre which is ligated by the four cysteine residues. Further towards the C-terminal region are a variety of other alignments that can be identified with regions of binding of FAD and NAD(P)H in NqrF and the flavoenzymes. The two regions R_{209}AYS and G_{242}IMSSY (boxes C and D) are likely to be associated with the binding of FAD. From the crystal structure of FNR [33,34], we may equate residues in box C with Arg^{93}, Tyr^{95} and Ser^{96} of FNR which form part of its FAD-binding pocket and residues in box D with Gly^{130} and Ser^{133} of FNR which anchor the pyrophosphate part of FAD. Further along the sequence alignment of Fig. 2 are two regions, G_{279}GGAGMAP (box E) and Y_{375}MCGPPMM (box F) that are likely to be associated with the binding of NAD(P)H. The residues in box E contain the type II′ xGxG turn of a characteristic NADPH-binding loop [34], whereas the YMCG sequence of box F is immediately followed by NAD(P)H-binding residues in FNR and its homologues [33].

Further regions of local possible homology may also be seen in the alignments of Fig. 2. For example, in the region of G_{261}PFGSF the two glycine residues and the proline are also conserved in FNR and homologues (equivalent to Gly^{149}, Gly^{152} and Pro^{150} in FNR), where their unusual bond angles provide an important structural domain [33]. We have yet to establish the significance of other possible domains.

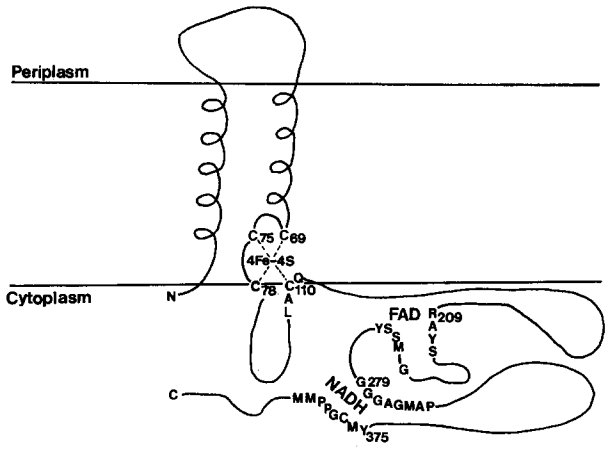

Fig. 3. Predicted folding model of the NqrF polypeptide and positions of redox centres.

We may, therefore, provisionally expect that the Na^+–NQR is composed of a relatively hydrophilic FP fragment of three subunits (NqrA, NqrC and NqrF), containing one FAD and one [4Fe-4S] iron sulphur centre on the NADH-oxidizing NqrF subunit, together with a hydrophobic HP fragment of three subunits (NqrB, NqrD and NqrE). The HP does not possess any obvious additional cofactor motifs but may act as a transmembrane anchor which incorporates the ubiquinone-binding site and possible sodium/proton channels between the iron sulphur centre and the membrane surfaces (see below). A lack of a motif for a second flavin group is consistent with our previous ability to identify only a single $n = 2$ redox potential ($E_{m,8} = -295$ mV and $n = 2$) in optical titrations of the flavin complement of the enzyme [20] and with the recent report [36] that only FAD is present in the purified enzyme.

3. Predicted folding model of the NqrF subunit

The information from hydropathy plots and sequence comparisons may be combined to produce a topological model of the NqrF subunit (Fig. 3). The subunit is likely to be anchored to the HP fragment by a hairpin pair of membrane-spanning α-helices in the N-terminal region. An iron sulphur centre resides in a domain close to the interface between this hydrophobic region and a large globular head which projects towards the cytoplasmic interior. This globular head has two further domains related to the structure of FNR [33], one providing the binding site for FAD and another providing the binding site for the NADH cofactor. In this model, both the N- and C-termini are expected to face the cytoplasm.

4. A model for coupled sodium ion translocation

Previous models for possible ion-coupling in this enzyme were based on an assumed cofactor composition of two flavins, FAD and FMN. Clearly, these ideas require reassessment in the light of the above analyses. Recently, we have outlined a model for proton translocation in the coupled iron/copper terminal oxidases which incorporates a general consideration of a rule of local electroneutrality of stable catalytic intermediates

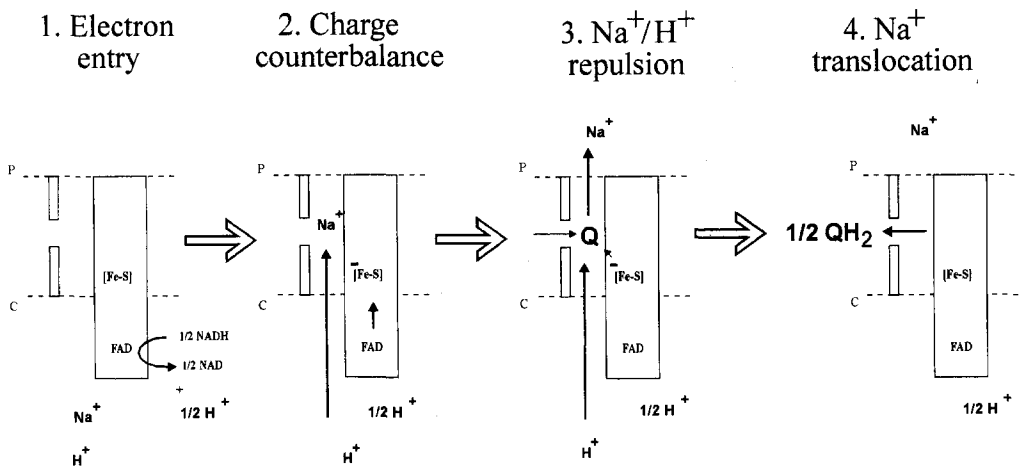

Fig. 4. A possible mechanism of ion/electron-coupling. See text for a description of individual steps.

[37,38]. When these intermediates are produced in a region of low dielectric strength, such charge neutralization occurs by counter-ion uptake. This consideration has been combined with the above structural considerations and our previous finding of a lack of sodium ion dependency of the midpoint potential of the FAD ([20], unpubl. data) to produce a new proposal for the essential features of coupling of electron transfer and sodium ion translocation in this enzyme (Fig. 4).

In this model, the iron sulphur centre is proposed to be in a relatively low dielectric environment such that electron transfer to it requires counter-ion uptake. It is proposed that the other subunits of this enzyme provide ion selectivity so that only sodium (or lithium) ions can provide such charge counterbalance (step 2). Binding of a quinone then results in electron transfer from the iron sulphur centre to quinone. The final quinol product of quinone reduction must, inevitably, become protonated (whether the quinol is formed by a dismutation of two semiquinone or whether there are two sequential electron transfers to the same bound quinone, remains a open point). Indeed, there will be a very strong driving force for such protonation, analogous to the driving force provided by oxide protonation to form water in the protonmotive oxidases [38]. The way in which this may be envisaged to drive net sodium ion translocation is shown in steps 3 and 4. The spatial orientation of the reactants results in an electrostatic repulsion by the proton of the sodium ion into the positive aqueous phase, resulting in the net translocation of sodium ions. It might be noted that the type of model outlined in steps 3 and 4 might also be considered as a basis for proton translocation in complex I, by substitution of an electronation-linked protonation of centre N-2 for the sodium-dependent steps.

It would be premature to speculate beyond this level until further details of net sodium/proton/electron-coupling ratios, semiquinone/quinol reaction products and subunit structures are established. Nevertheless, firm directions for future experimental investigations are clearly suggested by these considerations.

Acknowledgements: Purification of this enzyme, which led to subsequent N-terminal protein and, hence, gene-sequencing, was carried out during 1998–91 on an SERC-funded research grant to P.R. Rich (GR/F 78297). Subsequent work has been completed with a small temporary emergency fund provided by the Glynn Research Foundation. We are indebted to A.E. Jeal who carried out the digital analyses of protein sequences using a link to the SEQNET service at Daresbury.

References

[1] Fearnley, I.M. and Walker, J.E. (1993) Biochim. Biophys. Acta 1140, 105–134.
[2] Yagi, T., Yano, T. and Matsuno-Yagi, A. (1993) J. Bioenerg. Biomemb. 25, 339–345.
[3] Dupuis, A. (1992) FEBS Lett. 301, 215–218.
[4] Weidner, U., Geier, S., Ptock, A., Friedrich, T., Leif, H. and Weiss, H. (1993) J. Mol. Biol. 233, 109–122.
[5] Yagi, T. (1993) Biochim. Biophys. Acta 1141, 1–17.
[6] Yagi, T. (1991) J. Bioenerg. Biomemb. 23, 211–226.
[7] Moller, I.M., Rasmusson, A.G. and Fredlund, K.M. (1993) J. Bioenerg. Biomemb. 25, 377–384.
[8] Young, I.G., Rogers, B.L., Campbell, H.D., Jaworowski, A. and Shaw, D.C. (1981) Eur. J. Biochem. 116, 165–170.
[9] Xu, X., Koyama, N., Cui, M., Yamagishi, A., Nosoh, Y. and Oshima, T. (1991) J. Biochem. 109, 678–683.
[10] de Vries, S., Van Witzenburg, R., Grivell, L.A. and Marres, C.A.M. (1992) Eur. J. Biochem. 203, 587–592.
[11] Moore, A.L. and Rich, P.R. (1985) Encyclopaedia of Plant Physiology, Vol. 18 (Douce, R. and Day, D.A., Eds.) pp. pp. 143–172. Springer, Berlin, Germany.
[12] Moore, A.L., Bonner, W.D., Jr. and Rich, P.R. (1978) Arch. Biochem. Biophys. 186, 298–306.
[13] Unemoto, T., Tokuda, H. and Hayashi, M. (1990) Bacterial Energetics (Krulwich, T.A., Ed.) pp. 33–54. Academic Press, San Diego, CA.
[14] Unemoto, T. and Hayashi, M. (1993) J. Bioenerg. Biomemb. 25, 385–391.
[15] Skulachev, V.P. (1992) Molecular Mechanisms in Bioenergetics (Ernster, L., Ed.) pp. 37–73. Elsevier, Amsterdam, The Netherlands.
[16] Hayashi, M. and Unemoto, T. (1984) Biochim. Biophys. Acta 767, 470–478.
[17] Tokuda, H. and Unemoto, T. (1984) J. Biol. Chem. 259, 7785–7790.
[18] Hayashi, M. and Unemoto, T. (1987) Biochim. Biophys. Acta 890, 47–54.
[19] Asano, M., Hayashi, M., Unemoto, T. and Tokuda, H. (1985) Agric. Biol. Chem. 49, 2813–2817.
[20] Bourne, R.M. and Rich, P.R. (1992) Biochem. Soc. Trans. 20, 577–582.
[21] Beattie, P., Tan, K., Bourne, R.M., Leach, D., Rich, P.R. and Ward, F.B. (1994) FEBS Lett. 356, 333–338.
[22] Hayashi, M., Hirai, K. and Unemoto, T. (1995) FEBS Lett. 363, 75–77.

[23] Tan, K., Beattie, P., Leach, D.R.F., Rich, P.R. and Ward, F.B. (1996) Biochem. Soc. Trans. 24, 125.
[24] Nakamura, T., Komano, Y., Itaya, E., Tsukamoto, K., Tsuchiya, T. and Unemoto, T. (1994) Biochim. Biophys. Acta 1190, 465–468.
[25] Xu, X., Matsuno-Yagi, A. and Yagi, T. (1991) Biochemistry 30, 6422–6428.
[26] Xu, X., Matsuno-Yagi, A. and Yagi, T. (1992) Biochemistry 31, 6925–6932.
[27] Xu, X., Matsuno-Yagi, A. and Yagi, T. (1992) Arch. Biochem. Biophys. 296, 40–48.
[28] Xu, X., Matsuno-Yagi, A. and Yagi, T. (1991) Biochemistry 30, 8678–8684.
[29] Xu, X., Matsuno-Yagi, A. and Yagi, T. (1993) Biochemistry 32, 968–981.
[30] Karpel, R., Olami, Y., Taglicht, D., Schuldiner, S. and Padan, E. (1988) J. Biol. Chem. 263, 10408–10414.
[31] Ivey, D.M., Guffanti, A.A., Bossewitch, J.S., Padan, E. and Krulwich, T.A. (1991) J. Biol. Chem. 266, 23483–23489.
[32] Pinner, E., Padan, E. and Schuldiner, S. (1992) J. Biol. Chem. 267, 11064–11068.
[33] Karplus, P.A. and Bruns, C.M. (1994) J. Bioenerg. Biomemb. 26, 89–99.
[34] Karplus, P.A., Daniels, M.J. and Herriott, J.R. (1991) Science 251, 60–66.
[35] Correll, C.C., Batie, C.J., Ballou, D.P. and Ludwig, M.L. (1992) Science 258, 1604–1610.
[36] Pfenninger-Li, X.D. and Dimroth, P. (1995) FEBS Lett. 369, 173–176.
[37] Mitchell, R., Mitchell, P. and Rich, P.R. (1992) Biochim. Biophys. Acta 1101, 188–191.
[38] Rich, P.R. (1995) Aust. J. Plant Physiol. 22, 479–486.
[39] Harayama, S., Rekik, M., Bairoch, A., Neidle, E.L. and Ornston, L.N. (1991) J. Bacteriol. 173, 7540–7548.
[40] Harayama, S. (1991) J. Bacteriol. 173, 5385–5395.
[41] Harayama, S., Polissi, A. and Rekik, M. (1991) FEBS Lett. 285, 85–88.
[42] Higgins, D.G., Bleasby, A.J. and Fuchs, R. (1992) Comput. Appl. Biosci. 8, 189–191.